CHEMISTRY
A EUROPEAN JOURNAL

DOI: 10.1002/chem.200800606

Optical Properties of Hybrid Dendritic–Mesoporous Titania Nanocomposite Films

Eugenia Martínez-Ferrero,[a] Grégory Franc,[b] Serge Mazères,[c] Cédric-Olivier Turrin,[b] Cédric Boissière,[a] Anne-Marie Caminade,*[b] Jean-Pierre Majoral,*[b] and Clément Sanchez*[a]

Abstract: New hybrid optical sensors have been prepared by grafting specifically designed fluorescent, functionalised, phosphorus-containing dendrimers onto a nanocrystalline mesoporous titania thin film formed by evaporation-induced self-assembly. The structural characterisation and optical behaviour of these new fluorescent probes have been studied both in solution and after being grafted onto an inorganic network, which resulted in the discovery of improved probing selectivity in the solid state. This new hybrid sensor exhibits high sensitivity to phenolic OH moieties (especially those from resorcinol and 2-nitroresorcinol), which induce the quenching of fluorescence more efficiently in the solid state than in solution. This effect is a result of the increased spatial proximity of the fluorescent molecules, which is induced by pore confinement that makes the formation of hydrogen bonds between the hydroxyl moieties of the quenchers and the carbonyl groups of the dendrimer easier.

Keywords: dendrimers · fluorescent probes · hybrid materials · mesoporous materials · titania

Introduction

Dendrimers are highly branched macromolecules with interesting properties, the study of which constitutes an appealing field in the area of polymer science.[1] With tuneable chemical composition and size, these perfectly controlled structures are being developed more and more in the fields of materials science, catalysis and biology. In materials science, dendrimers participate in the elaboration of complex hybrid organic–inorganic functional nanoarchitectures. Due to the presence of specific functional groups at their surface or in their internal cavities, they can act as controlled pockets when embedded in a mineral matrix. In such a configuration, they can act as sensitive probes, selective adsorbents, drug-release controllers or nanoreactors.

As well as purely organic dendrimers, the phosphorus-containing dendrimers also excel because of their simple synthesis, their diverse chemistry and their easy attachment to coupling agents that are able to form strong bonds with inorganic materials. These striking features permit their use in hybrid materials either as building blocks or by creating supramolecular assemblies on the surface of materials.[2] The first hybrid materials, prepared in 2000, were made by the co-condensation of phosphorus dendrimers with a silica-based inorganic matrix, which gave rise to porous materials that tend to be used as absorbents or insulating materials.[3] *S*econd-generation hybrid materials were obtained shortly afterwards by using non-silicate matrices. Two synthesis approaches have been tested: First, the co-assembly of preformed nano building blocks (NBB), that is, $[Ti_{16}O_{16}(OEt)_{32}]$

[a] Dr. E. Martínez-Ferrero, Dr. C. Boissière, Dr. C. Sanchez
Laboratoire de Chimie de la Matière Condensée
Université Pierre et Marie Curie
4 Place Jussieu
75252 Paris Cedex 05 (France)
Fax: (+33) 144-274-769
E-mail: clems@ccr.jussieu.fr

[b] Dr. G. Franc, Dr. C.-O. Turrin, Dr. A.-M. Caminade, Dr. J.-P. Majoral
Laboratoire de Chimie de Coordination du CNRS
205 Route de Narbonne
31077 Toulouse cedex 4 (France)
Fax: (+33) 561-553-003
E-mail: caminade@lcc-toulouse.fr
majoral@lcc-toulouse.fr

[c] Dr. S. Mazères
Institut de Pharmacologie et de Biologie Structurale
CNRS-UPS, UMR 5089
205 Route de Narbonne
31077 Toulouse cedex 4 (France)

Supporting information for this article is available on the WWW under http://dx.doi.org/10.1002/chem.200800606 or from the author. It contains the X-photoelectron spectroscopy studies of dendrimer **7** and TiO_2–**7** (Figure S1), and the FTIR spectrum of TiO_2–**7** quenched by 4-nitrophenol (Figure S2).

clusters and dendrimers, gave rise to bicontinuous mesostructured hybrid gels formed from periodically stacked inorganic and organic NNBs.[4] Second, the mix of dendrimers with titanium and cerium alkoxides allowed the control of the reactivity of the inorganic precursors. After the appropriate treatments, porous materials made of dendrimers locked in metal-oxide matrices were obtained.[5]

For surface modification purposes, the main advantage of using dendrimers instead of simple monomers is the number of anchoring points provided by the dendrimer, which enhances the stability of the interfaces and give them a controlled roughness. In particular, these properties were used for the elaboration of stable and sensitive DNA chips.[6]

For optical applications, the dispersion of fluorescent dendrimers in a hole-conducting polymer has permitted the preparation of organic light-emitting diodes.[7] Fluorescent dendrimers are also used for other applications, such as analytical probes, organic nanodots or biological labelling.[8] In these functions, they can act as sensors by monitoring the fluorescence response of the active entities. For example, hazardous nitrophenols are known to be good quenchers of some fluorescent substances due to their electron acceptor capacity.[9] Hence, specifically functionalised dendrimers have vast potential as components for the construction of detectors.

However, practical detector applications require that the probe should be immobilised into a robust matrix with a high surface area so that high sensitivity is reached and the fast diffusion of the analytes is allowed. For this application, micellar-templated materials (MTS) prepared by the sol-gel route constitute a new type of extremely interesting matrix for dendrimer immobilisation, due to their highly organised and easily accessible 2D or 3D mesoporous structures and huge surface area.[10] The recently developed evaporation-induced self-assembly method permits their preparation in different forms, such as nanometric powders, monoliths, fibres and especially thin films of optical quality and controlled thickness.[11] These outstanding properties make these compounds the ideal candidates for preparing new multifunctional hybrid organic–inorganic optical sensors. However, as demonstrated recently, the usual silica MTS have poor stability versus humidity.[12] A possible alternative is to use MTS films made of amorphous (or more ideally nano-crystalline) transition-metal oxides, such as TiO_2, ZrO_2 or Al_2O_3, or mixed metal oxides that are mechanically and chemically much more stable.[13]

Herein, we report the synthesis of new hybrid optical sensors shaped as thin films. For the inorganic matrix, we selected nano-crystalline titania mesostructured films that present excellent chemical stability[14] and an ordered grid-like porous network that provides good accessibility and permeability for external species.[15] Within these films, we grafted new fluorescent phosphorus-containing dendrimers, which have been specially designed to fulfil two key properties: First, to incorporate a reactive phosphonate group that can graft onto titanium oxide mesoporous films, but that would not impair the fluorescence properties, and second, to show a well-defined fluorescence pattern and thus behave as a fluorescent organic probe for different hazardous nitrophenols and phenols. To compare grafting and detection efficiency, we also used $(ZrO_2)_x(SiO_2)_{1-x}$ MTS films with a 3D mesoporous network as an alternative substrate. The study of the optical properties of these systems was performed by using quenching tests to determine the behaviour of the dendrimers in the solid state and compare the results with those obtained in solution.

Results and Discussion

Dendrimer synthesis and characterisation: As stated in the introduction, the dendrimer-like structures described herein were specially designed to have two non-interfering functionalities: First, to act as fluorescent probe, and second, to possess distinct phosphorylated functional groups dedicated to the strong anchoring of the dendrimers at the TiO_2 surface. In this regard, some of our previous studies reported that the versatile functionalisation of cyclotriphosphazene core dendrimers is a valuable route to functional dendritic precursors, either for the design of fluorescent dendrimer cores[16] or for the design of unprecedented divergent points.[17] The synthesis of the dendrimer is shown in Scheme 1. The first step in building the desired core consists of the reaction of one equivalent of the sodium salt of 4-hydroxybenzaldehyde with $N_3P_3Cl_6$ to give rise to a monosubstituted focal point (**1**).[18] The ^{31}P NMR spectrum of **1** shows one triplet at $\delta = 11.73$ ppm ($^2J(P,P) = 62.4$ Hz) for the phosphorus with the aldehyde derivative and one doublet at $\delta =$ 22.53 ppm for the other two phosphorus atoms, which confirmed the formation of the desired structure. In parallel, the maleimide-based phenolic chromophore **2** was synthesised under the usual conditions (AcOH and high temperature)[19] from tyramine and diphenyl maleic anhydride (see Scheme 1). Compound **2** was obtained in very good yield (95%), which lead us to perform the same procedure with phenylethylamine to prepare the same compound without the OH group (**3**; 98% yield) to measure differences in the fluorescence properties.

The substitution of the five remaining chlorine atoms of **1** by chromophore **2** under the usual conditions (THF and Cs_2CO_3, 2 equiv per chlorine) gave **4**. The reaction is relatively slow and needs 2 days to complete, as shown by ^{31}P NMR spectroscopic monitoring (multiplet at $\delta =$ 8.47 ppm). After work-up, the purity of the dendrimer was also confirmed by ^1H, ^{13}C NMR and FTIR spectroscopies and mass spectrometry. At this point, the ^1H and ^{13}C NMR spectra started to show multiple signals due to the unsymmetrical arrangement of the branches around the core. A good example to describe this phenomenon concerns the ^1H NMR spectrum of the tyramine moiety, in which each methylene group gave two multiplets at $\delta = 2.99$ ($C^{a'}$–H) and 3.87 ppm ($C^{b'}$–H) in its instead of two triplets. Two different signals for each carbon also appear in the ^{13}C NMR spectrum at $\delta = 33.96$ and 33.99 ppm for ($C^{a'}$) and at $\delta =$

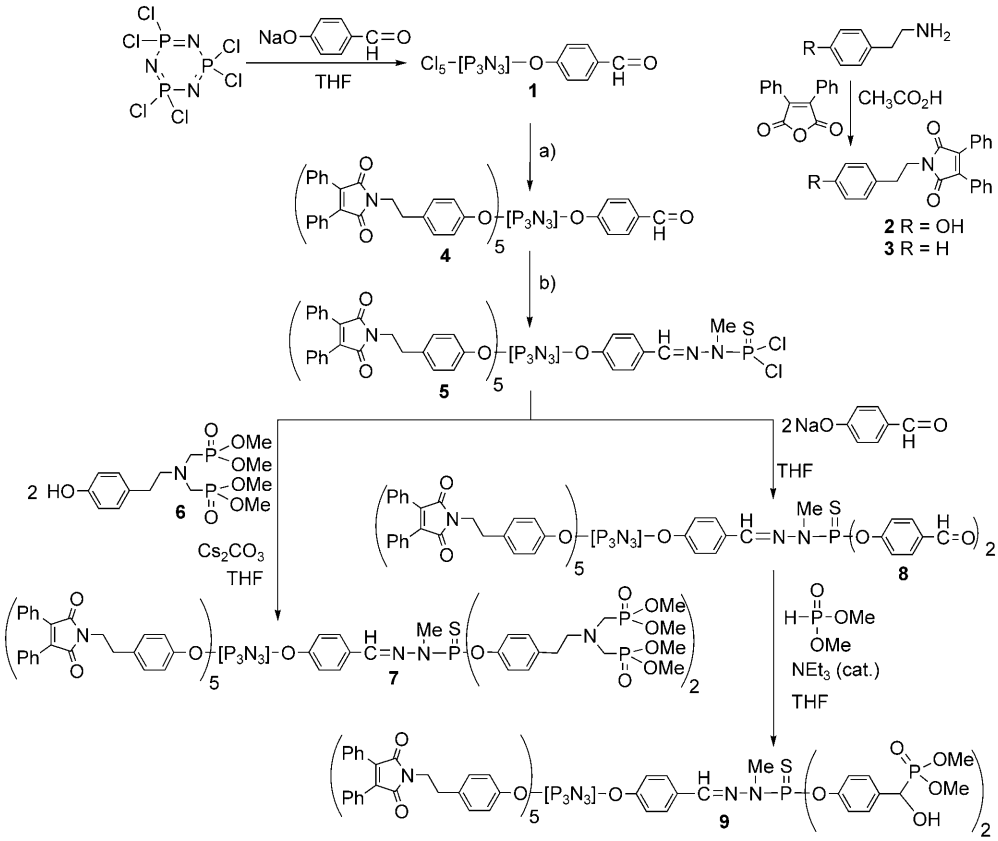

Scheme 1. The synthesis of chromophores **2** and **3** followed by the synthesis of fluorescent anchorlike dendrimers **7** and **9**. a) **2** (5 equiv), Cs_2CO_3, THF. b) $H_2NNMeP(S)Cl_2$, $CHCl_3$.

39.51 and 39.54 ppm for ($C^{b'}$), respectively (see the Experimental Section for the atom labelling system).

The dendritic core **4** was then functionalised to allow further grafting onto the mesoporous films. Phosphonate was chosen as the grafting entity because it is known to form stable compounds with metal oxides.[20] Therefore, and to have accessible grafting functional groups, we decided to grow the specific branch with the aldehyde up to the first generation. Thus, the next step consisted of a condensation between the main structure and one equivalent of *N*-methyldichlorophosphorhydrazide. This condensation reaction was monitored by ^{31}P and ^{1}H NMR spectroscopies that indicated the total disappearance of the signal from the aldehyde group, but FTIR spectroscopic monitoring could not be performed because the carbonyl of the maleimide at 1703 cm^{-1} strongly hides the signal of the aldehyde group. This step gave the dendritic core **5**, with the $P(S)Cl_2$ end group appearing in the ^{31}P NMR spectrum at $\delta = 63.02$ ppm, whereas the phosphazene core remained unaffected. The molecule has an unsymmetrical architecture, as shown, for example, by two signals at $\delta = 170.51$ and 170.53 ppm in the ^{13}C NMR spectrum for the carbonyl groups of the maleimides. Following this, nucleophilic substitutions of the chlorine atoms by **6**[16] gave **7** in very good yield (83%). After purification, the chemical shifts of the ^{31}P NMR spectrum appeared at $\delta =$ 8.66 ppm for the core signal, $\delta = 26.89$ ppm for the phosphonate moieties and $\delta = 63.10$ ppm for the P(S) group. Asymmetry remained visible in the ^{1}H and ^{13}C NMR spectra, with multiple signals for the methylene groups of the tyramine moieties.

Hydroxyphosphonate is also a good candidate as a grafting functional group on metal oxide, and was thus used on the $(ZrO_2)_x(SiO_2)_{1-x}$ films. Consequently we slightly modified our strategy to reach this other target; in fact, a two-step process starting from **5** readily gave access to this new compound. First, aldehyde extremities (see compound **8**) were attached in a simple manner by nucleophilic substitution of the chlorine atom with the sodium salt of 4-hydroxybenzaldehyde. Second, a classic Abramov-type reaction is undertaken with **8** in presence of dimethylphosphite in a concentrated THF solution, which leads to the desired compound **9** with two α-hydroxyphosphonates on the surface.[21] Finally, ^{1}H NMR spectroscopy and TLC were used to ascertain the purity and the absence of residual impurities. Moreover, compounds were subjected to flash column chromatography when possible during the synthesis to remove impurities.

The emissive properties of each resulting compound have been characterised in solution by UV/Vis absorption spectroscopy and fluorescence measurements in distilled CH_2Cl_2, and are summarised in Table 1. Note that the absorption increases proportionally as the number of fluorescent groups

Table 1. Emissive properties of synthesised fluorescent molecules **2–4** and **7–9** in CH_2Cl_2.

	ε [$mol^{-1}cm^{-1}$]	λ_{ex} [nm]	λ_{em} [nm]	Φ[a] [%]
2	3457	320/380	506	8
3	3470	300/375	506	52
4	17000	300/375	506	64
7	17650	315/375	506	50
8	18900	307/376	506	61
9	17900	302/375	506	52

[a] Coumarine 6 ($\Phi = 78\%$ in EtOH) was used as the reference compound.

increases. They all possess two excitation centres, one for the phenyl groups around $\lambda = 300$–320 nm and another at $\lambda = 375$ nm for the maleimide moiety, which lead to a single emitting species at $\lambda = 506$ nm because the chromophore has a π-conjugated system. Another important point concerns the quantum yields that were calculated with Coumarine 6 as the reference ($\Phi = 78\%$ in EtOH). The quantum yields of monomers **2** and **3** were calculated to be 8 and 52%, respectively. Therefore, the lack of an OH group for **3** enhances the fluorescence emission, which suggests that this specific group self-quenches the emission of **2**.[22] Therefore, the dendrimers have moderate to good quantum yields that permit the formation of the fluorescent hybrid materials.

Structural characterisation of the functionalised films: The mesoporous titania films were functionalised by dip-coating in a dilute 1 mM solution of dendrimer **7** in dichloromethane under an air flux at 40°C, to give TiO_2–**7**. This technique permits the homogeneous introduction and deposition of the organic molecules inside the films, and the evaporation of the solvent. Further washing in dichloromethane removed non-bonded dendrimers. Because the phosphonates are known to give rise to covalent bonds with titanium oxide,[23] we can easily prepare functionalised films in this way.

Transmission electron microscopy (TEM) reveals that the films consist of an ordered structure, in which gridlike porous structures, aligned parallel to each other, stand perpendicular to the substrate (see a TEM top view in Figure 1a) and the walls are composed of 10 nm anatase nanocrystals, in accordance to previous published results (see the diffraction pattern in Figure 1a, inset).[24,25] The structural characterisation was completed by using environmental ellipsometric porosimetry (EEP), which is based on the measurement of water adsorption–desorption isotherms. Figure 1b shows the variation of the normalised volume of adsorbed water into the film (V_{ads}/V_{film}), which is directly proportional to the porous volume, with the relative water pressure (P/P_0). As the relative humidity (RH) increases to 70%, the non-functionalised titania film takes up water slowly. Above 70% RH, a massive adsorption of water was observed, which is characteristic of the narrow pore-size distribution of these mesostructured matrices.[24–26] Upon desorption, the isotherm exhibits a hysteresis owing to the presence of restrictions between the mesopores of the films. Data are well fitted between 500 and 1000 nm with a

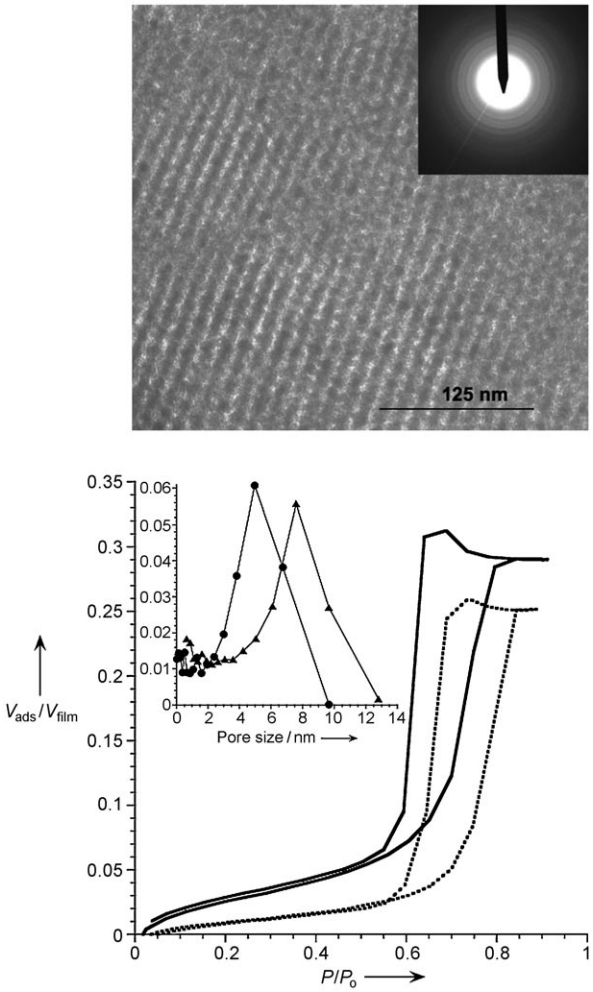

Figure 1. Top: TEM image of the mesoporous films after being heated at 550°C; inset: the diffraction pattern. Bottom: Comparison of water adsorption–desorption isotherms obtained from EEP measurements for the TiO_2 (——) and TiO_2–**7** (•••••) films. Inset: pore-size distributions for the TiO_2 (▲) and TiO_2–**7** (●) films, obtained from the adsorption region of the isotherm.

Cauchy single-layer model, which indicates that the composition of the film is homogeneous. The parameters of the porous network were calculated from the isotherm (Table 2) by considering that mesopores are anisotropic and connected with nearest neighbours by four restrictions.[26] Data collected from functionalised films were perfectly fitted with the same model (a single-layer model), which suggested that the organic molecules were homogeneously dispersed within the film, and that no extra layer of dendrimers was detecta-

Table 2. Comparison of the structural parameters of the TiO_2 and TiO_2–**7** films.

	Thickness [nm]	Small pore axis [nm]	Large pore axis [nm]	Porous fraction [%]	Water contact angle [°]
TiO_2	197	4.5	7.6	29	5±2
TiO_2–**7**	197	3.0	5.0	25	60±2

ble on the top of the TiO_2 layer. The isotherms display a similar behaviour to that of the titania film. However, the introduction of the dendrimers resulted in a porous network with a decreased pore size (from 7.6 to 5.0 nm for ungrafted and grafted TiO_2, respectively) and a decreased porosity (from 29 to 25%). These data are coherent with the known flattening of dendrimers on surfaces.[1b] In addition, static water contact-angle measurements proved that the high hydrophilicity of the TiO_2 surface was lost upon dendrimer grafting (Table 2). This strongly suggests that the surface hydroxyl groups of titania were barely accessible after grafting. From the comparison of the parameters shown in Table 2, we can conclude that functionalisation does not alter the thickness or the meso structure of the film.

The presence of dendrimers in the films has also been verified by FTIR spectroscopy, which compares the spectra of functionalised and non-functionalised samples in different regions (Figure 2). Between $\tilde{\nu}=3600$ and 2600 cm^{-1} (Figure 2a), we observed a broad signal at $\tilde{\nu}=3420$ cm^{-1} due to the hydroxyl groups on the surface of the titania film. After the introduction of the organic dendrimer, the broader signal is centred at $\tilde{\nu}=3300$ cm^{-1} and was assigned to the contribution from the remaining hydroxyl groups of the inorganic matrix. The weak band centred at $\tilde{\nu}=3050$ cm^{-1} was assigned to the aromatic alkene groups and the bands at $\tilde{\nu}=$ 2963, 2927 and 2855 cm^{-1} are due to the $-CH_2-$ groups from the organic molecules. At lower wavelengths (Figure 2b) we observed bands at $\tilde{\nu}=1275$, 1206, 1200, 1184, 1164, 1108, 1063 and 1030 cm^{-1} on the functionalised films, which were assigned to the dendrimer. From this examination, we have attempted to identify the bonding mode between the organic dendrimer probe and the titania film. Previous work using phosphonate coupling molecules grafted to titania nanoparticles showed that the appearance of P–O bands is evidence for extensive condensation and coordination of the phosphoryl oxygen, which mainly leads to bidentate phosphonate units.[23] Consequently, we have focused our analysis on the $\tilde{\nu}=1000$–1350 cm^{-1} region, as shown in Figure 2c, which displays the spectra of the functionalised film and the free dendrimer. Although they look quite similar, the band that appears at $\tilde{\nu}=1030$ cm^{-1} in the spectrum of dendrimer **7** is overlapped in the spectrum of the TiO_2–**7** film by new, broad bands at $\tilde{\nu}=1002$, 1018, 1045, 1055 and 1065 cm^{-1} that were assigned to P–O stretching bands, in agreement with previously published work.[23]

In addition, and to shed more light on this subject, we also performed X-photoelectron spectroscopy (XPS). The survey of the dendrimer and the functionalised titania film (see the Supporting Information) displays the expected peaks for O, C, N and P (plus Ti for the film), which strongly supports the presence of dendrimer in the films. A closer analysis of the O1s region of the spectra did not afford unambiguous proof of the covalent bonding of the dendrimers onto the surface (Figure 3). According to literature, P–O–Ti covalent-bond formation can be followed by observing the evolution of P–O–Ti (531.4 eV) and P–OH (533 eV) peaks.[27] Pure dendrimer **7** displays three adjacent peaks at

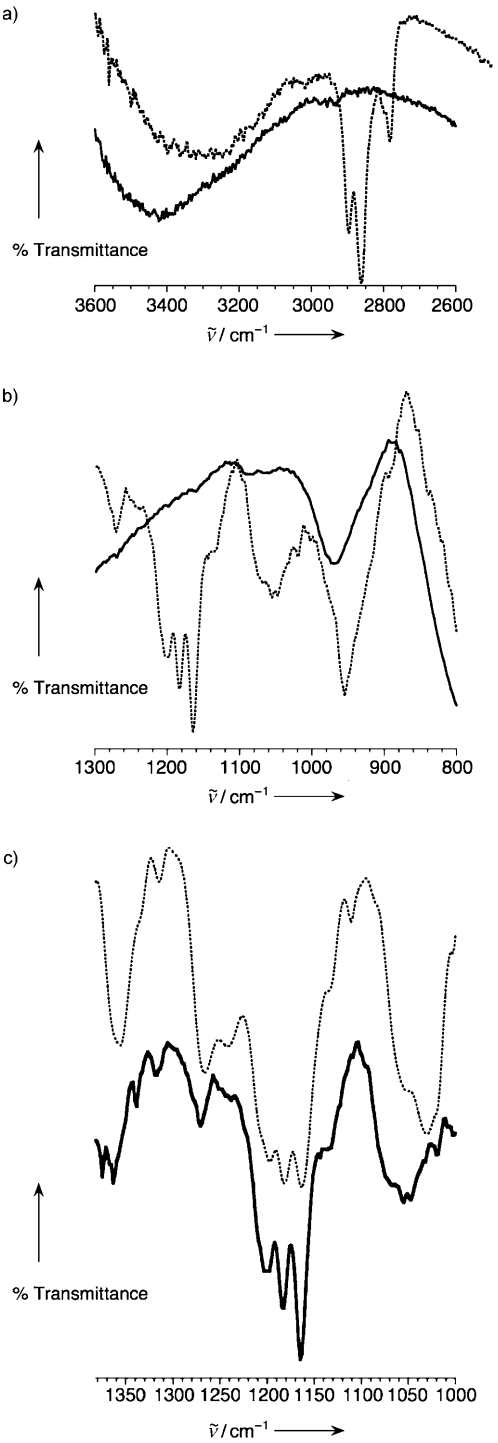

Figure 2. FTIR spectra between a) 3600 and 2600 cm^{-1} and b) 1300 and 800 cm^{-1} of the TiO_2 (——) and TiO_2–**7** (•••••) films. c) FTIR spectra of free dendrimer **7** (•••••) and TiO_2–**7** (——) between 1000 and 1350 cm^{-1}.

533.6, 532.08 and 529.43 eV. In our case, the functional groups that are able to react with the inorganic network are P–O–CH_3 and P=O. The literature binding energies of these groups range from 531.3 to 532.5 eV.[27] The contribution from the additional oxygen of the C=O groups (532 eV) to the same peak makes the separation of P–O–CH_3 and C=O

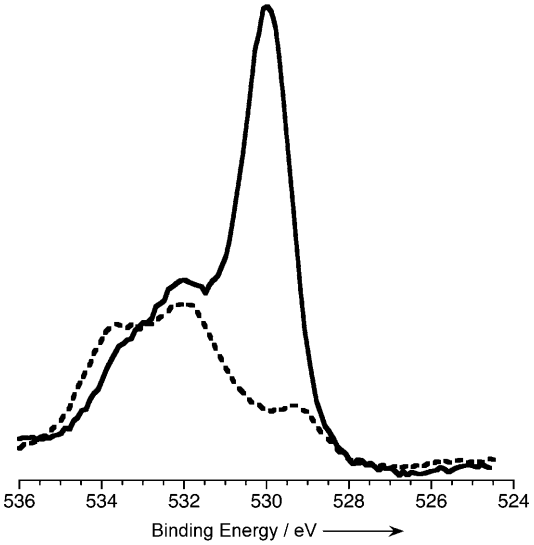

Figure 3. XPS spectra showing the O1s signals of the TiO_2–**7** film (——) and free dendrimer **7** (•••••).

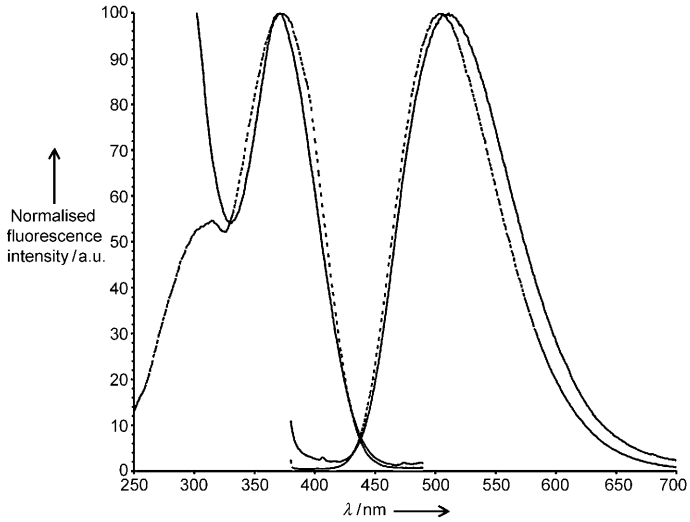

Figure 4. Normalised fluorescence spectra of the TiO_2–**7** film (——) and dendrimer **7** (•••••) in solution. Left: excitation spectrum after emission at 520 nm and right: emission spectrum after excitation at 370 nm.

signals difficult. Upon functionalisation, the intense peak at 529.7 eV from TiO_2 and the broadening of the two high-bonding-energy peaks of dendrimer **7** make the P–O–Ti (531.4 eV) contribution difficult to detect.

Finally, the measurement of the water-contact angle of films functionalised with dendrimer solutions of different concentrations shows that higher angles are obtained for higher solution concentrations (results not shown). However, after washing in dichloromethane and drying, the resulting angle was the same for all the samples. Similarly, the refractive indices of the impregnated films after washing were found to be constant. Thus, we deduced that the final concentration of organic molecule that remained in the films was the same regardless of the concentration of the initial dendrimer solution.

From the EEP, FTIR and XPS measurements, we corroborated the presence of the dendrimer inside the films, but definite proof of the covalent grafting of dendrimers onto the TiO_2 surface could not be obtained. However, there are many examples in the literature of grafting under similar conditions that attest the formation of covalent bonds between TiO_2 surfaces and phosphonate functional groups.[23,26,28] Therefore, we have assumed herein that the dendrimers are covalently bonded to the inorganic framework.

Optical properties of the functionalised films: The films were characterised by steady-state fluorescence (Figure 4). The excitation spectrum of the dendrimer in solution shows two maxima at $\lambda = 315$ and 375 nm that are due to the phenyl and the maleimide moieties, respectively, whereas the emission maximum is at $\lambda = 506$ nm. The corresponding spectra of the solid-state samples show similar trends to those in solution, although the maxima are slightly red-shifted to $\lambda = 373$ and 515 nm, which is attributed to the bonding of the dendrimer to the titania network. Energy transfer is observed between titania and the dendrimer, a phenomenon that has been previously reported in sol-gel-derived hybrid (organic dye) titania matrices.[29] It is likely to be associated with the partial overlap between the high-energy absorption band of the dendrimers and the phosphonate-complexation-driven shift in the band gap of titania.

The influence of quenchers: The fluorescent emission of the dendrimers is very strong even after functionalisation, which makes these devices quite attractive for use as sensors. For that reason, we performed quenching experiments at room temperature to understand their optical properties. The functionalised films were dipped into stock solutions of different compounds (see Scheme 2 and Table 3 for details) and then dried in air. To verify the homogeneity and stability of the hybrid films during the experiments, EEP, FTIR

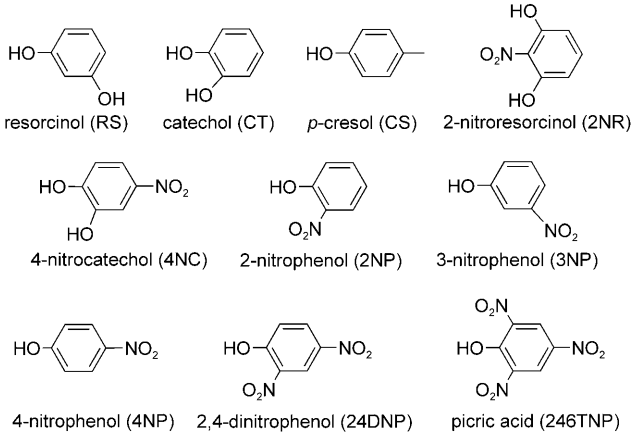

Scheme 2. Molecular structure of the quenchers used herein.

Table 3. Quenching molecules used in the fluorescence tests of the TiO_2–**7** films, with the reaction conditions and the results for both the solid-state and solution phases, from + (moderate) to +++++ (very strong).

Quencher	Conditions	Quenching response (solid state)	Quenching response (solution)
2NP	10 mM, $CHCl_3$	++	++++
3NP	10 mM, $CHCl_3$	+++	+
4NP	10 mM, $CHCl_3$	++	+
24DNP	10 mM, EtOH	++	–
246TNP	10 mM, EtOH	+++	–
2NR	10 mM, $CHCl_3$	+++++[a]	++
4NC	10 mM, EtOH	++	–
RS	10 mM, EtOH	+++++	–
CT	10 mM, EtOH	++++	–
CS	10 mM, $CHCl_3$	++++	0
water	–	+	–
1-pentanol	–	+	–
ethanol	–	0	–

[a] See Figure 6.

and contact angle measurements were performed at each step.

The first test was performed in water to determine the sensitivity of the devices towards humidity. Soaking and drying the film had a quenching effect that moderately modified the initial fluorescence values, as shown in Figure 5. This is attributed to the formation of hydrogen bonds between water and the carbonyl groups of the dendrimers, as observed previously with chromophores **2** and **3** in solution (see above). To explore this effect, we also tested a range of alkyl alcohols and obtained different results. Tests with 1-pentanol produced the same quenching effect, which confirmed our first observations. However, ethanol did not quench the fluorescence, probably because to its higher volatility. $CHCl_3$ was our solvent of choice, however this surprising result permitted us to use ethanol as well, as an alternative solvent for testing the quenching potential of molecules that are insoluble in $CHCl_3$.

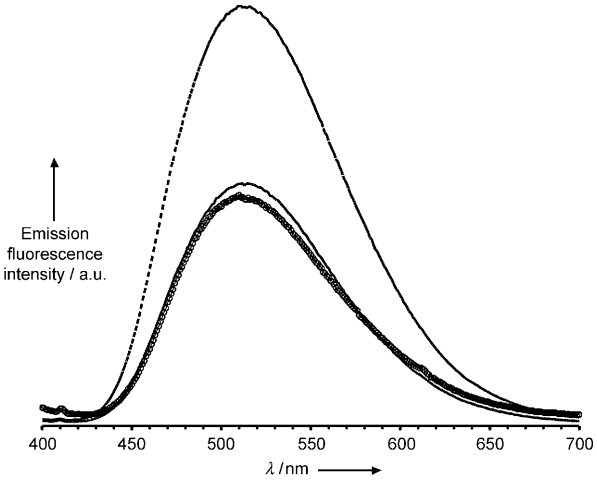

Figure 5. The effect of water (○) and 1-pentanol (——) on the fluorescence emission ($\lambda_{ex}=373$ nm) of TiO_2–**7** (-----).

Once the effect of OH moieties had been established, we tested hazardous molecules that contain this group. Therefore, we studied the response of our hybrid sensor to several nitrophenol derivatives and observed spectacular modifications of the fluorescence (see Table 3). Hazardous 2-nitrophenol (2NP), 4-nitrophenol (4NP) and 2,4-nitrophenol (24NP) have a stronger quenching effect on the fluorescence of the dendrimer than water and pentanol. 3-Nitrophenol (3NP) and 2,4,6-trinitrophenol (246TNP) presented a stronger quenching effect, although the presence of water in the latter reactant should be taken into account. Molecules containing various phenols, such as 2-nitroresorcinol (2NR) and 4-nitrocatechol (4NC), behaved in the same manner; 2NR demonstrated the best quenching response. Finally, we tested parent molecular structures containing no nitro groups to determine their influence on quenching. As expected, *p*-cresol (CS), resorcinol (RS) and catechol (CT) showed the same quenching tendency previously observed. RS had the strongest quenching effect determined in this study (see Figure 6), with less than 1% of fluorescence remaining. Therefore, the hybrid material behaves as an excellent sensor for resorcinol and 2-nitroresorcinol.

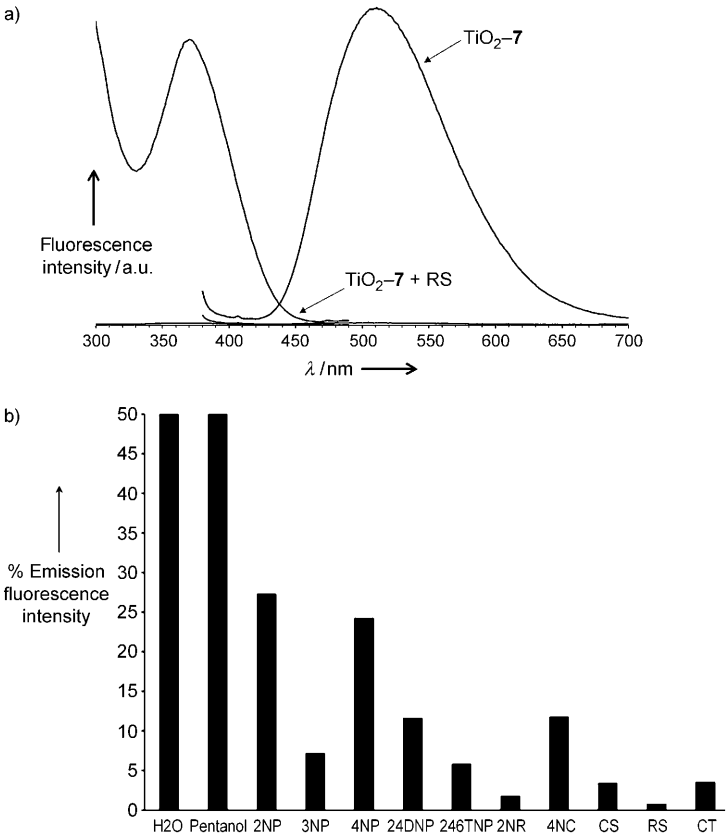

Figure 6. a) Modification of the fluorescence response ($\lambda_{ex}=373$ nm, $\lambda_{em}=520$ nm) of the TiO_2–**7** film after soaking for 10 min in a 10 mM solution of resorcinol in $CHCl_3$ (TiO_2–**7**+RS). b) Percentage of fluorescence remaining after the quenching experiments.

The results suggest that the fluorescence variation is due to the interaction of the carbonyl group of the dendritic core with the phenolic OH group. Indeed, the fluorescence spectra of the hybrid films displayed no shift in the maximum of the emission wavelength. This observation suggests that neither π stacking nor excimer formation occurs within the dendritic-like structure. To shed light on this hypothesis we measured the quenched films by using FTIR (see the Supporting Information, Figure S2). The band at 1705 cm^{-1}, which was assigned to the carbonyl group of the maleimide moiety, broadens and shifts towards lower frequency values (between $\tilde{\nu}=1700$ and 1690 cm^{-1}, depending on the quencher), as expected for the formation of a hydrogen bond between the maleimide carbonyl and the phenolic OH group of the quenching molecule.[30] In addition, UV/Vis spectroscopy measurement of the quenched hybrid material displays a hypsochromic shift of approximately 10 nm. The fact that water and alkyl alcohols, such as pentanol, affect the fluorescence in the same manner supports this idea.

We also tested the reversibility of the quenched system under different conditions. The use of a protic polar organic solvent like ethanol, with or without refluxing conditions, did not give positive results. Washing attempts with acidic water (one night at pH 0.3) resulted in the recovery of 40% of the fluorescence initial values but, unfortunately, the films deteriorated during the experiments. Less acidic solutions gave poor signal recovery results. Basic conditions gave the best results, with a fluorescence recovery of 60% of the initial intensity while maintaining film homogeneity. In Figure 7, the evolution of fluorescence intensity with different pH values for 2NR shows that a partial fluorescence recovery starts at pH 9 and reaches a maximum at pH 10. Given that water alone quenches between 40 and 50% of the initial "dry film" fluorescence (Figure 5), these basic pH recovery rates are very satisfactory.

Additionally, we performed measurements on functionalised $(ZrO_2)_x(SiO_2)_{1-x}$ ($x=0.1$ or 0.2) films with fluorescent dendrimer **9** and observed the quasi-complete disappearance of the fluorescence intensity after excitation at $\lambda=370$ nm. This can be explained by the presence of a higher density of acidic hydroxyl groups bonded to the silicon and zirconium centres of the amorphous inorganic network, which may interact with the maleimide moiety by hydrogen bonding. Additionally, the excitation of the phenyl moiety ($\lambda=290$ nm) gives a weak fluorescent signal, which demonstrates that, in these amorphous matrices, the fluorescent centres of the dendrimers are more affected by the hydroxyl groups from the surface than from within the TiO_2 nano-crystalline film.

Comparison of optical properties and advantages of the hybrid material: Once the hybrid devices were characterised, we focused our attention on dendrimers in solution. For that, fluorescent dendrimer **8** (with aldehyde extremities) was tested with the quenchers that are soluble in dichoromethane, namely 2NP, 3NP, 4NP, 2NR and CS, by following the Stern–Volmer procedure. In addition to an initial solution of **8** (0.138 μM) in distilled dichloromethane, small

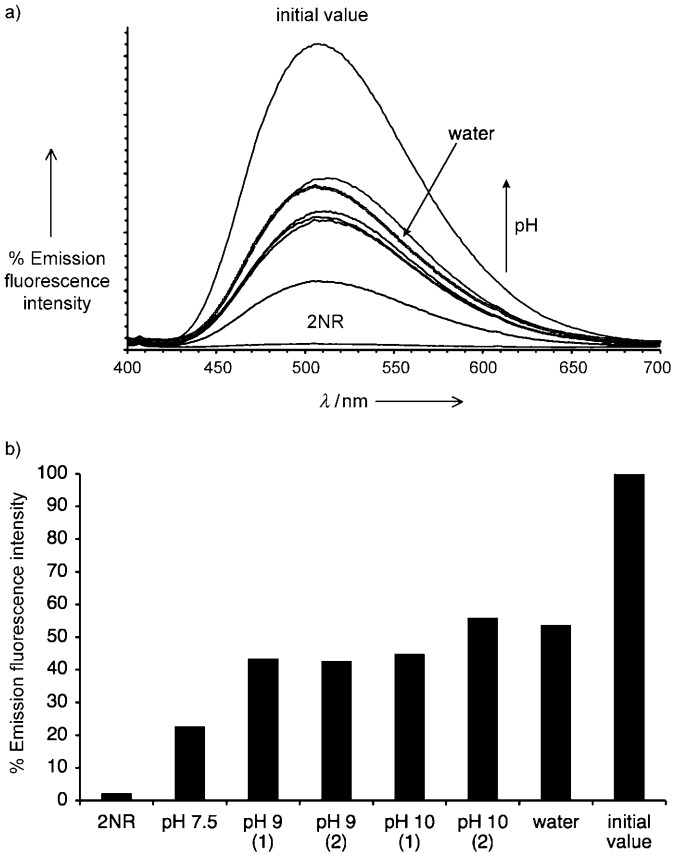

Figure 7. a) Evolution of the fluorescence emission ($\lambda_{ex}=373$ nm) of quenched TiO_2–**7** devices after soaking in basic aqueous solutions with pH values from 7.5 to 10. Results in water have been included for comparison purposes. b) Percentage of fluorescence recovery with pH for 2NR. Two consecutive measurements were performed for pH 9 and 10.

quantities of an identical solution of **8** that also contained the quencher in higher concentrations were required, the modification of the fluorescent emission by dilution being negligible. The results, which are shown in Figure 8, clearly reveal that there is no quenching effect in solution, except for 2NP and for 2NR (only moderately).

Therefore, and in agreement with previous observations,[31] the hybrid material exhibits a strong improvement in sensitivity. This can be explained by a local concentration of dendrimer in the porous volume that is much higher than a dispersion of the same quantity of dendrimers in solution in dichloromethane. Indeed, when the phenol groups of the dendrimer interact with the carbonyl groups on the surface of the hybrid material, the probability of a phenyl group to interact with another C=O bond or with the TiO_2 surface—and hence to become trapped through hydrogen bonding with neighbouring dendrimers—is much higher in a confined volume than in solution. As a consequence, we assumed that grafted dendrimers behave like a supported phase that can concentrate the probes because a partition coefficient exists between the dendrimer and the solvent. Therefore, although the interaction between the quencher carbonyl groups and the dendrimer hydroxyl groups remains the same in solution

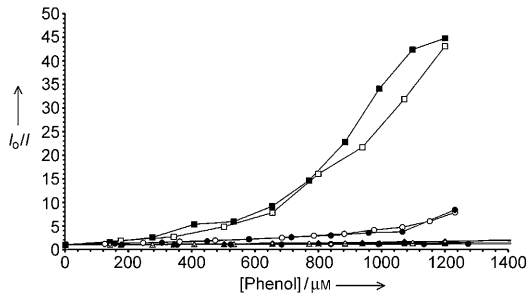

Figure 8. The Stern–Volmer procedure for dendrimer **8** in solution (0.138 μM) and quenching solution (**8**, 0.138 μM and quencher, 1 mg mL^{-1}). We performed two tests for each compound and all tests were performed in CH_2Cl_2. □,■: 2NP (10 mg/10 mL), △,▲: 3NP (10 mg/10 mL), ◇,◆: 4NP (10 mg/10 mL), ○,●: CS (10 mg/10 mL), ○,●: 2NR (10 mg/10 mL).

and in the solid state, the device gives statistically more chances to create the hydrogen bond that extinguishes the fluorescence of the dendrimers.

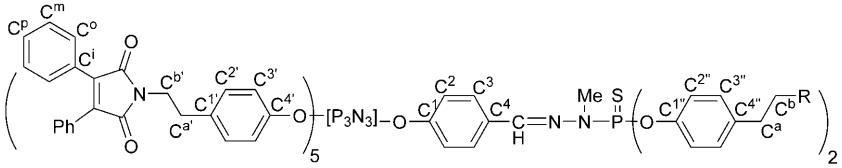

Scheme 3. Atom labelling system used for NMR spectral assignments.

Conclusion

Herein, we reported the construction of a hybrid material composed of fluorescent dendrimers anchored to nanocrystalline mesoporous titania thin films, which provides the first example, as far as we know, of such a compound. The new fluorescent dendrimers have been specifically designed to act as fluorescent probes and to be grafted to the substrate. At the same time, titania films offer the perfect environment for the grafting of the organic molecules due to their chemical composition and stability, their mesoporous cavities and their optical properties that do not interfere with those of the dendrimers.

The characterisation of these new hybrid mesostructured films has demonstrated that they have fluorescent properties. The dendrimers grafted to the films display higher quenching efficiency towards phenolic OH moieties (especially those from resorcinol and 2-nitroresorcinol) than in solution. This effect is attributed to the increased spatial proximity of the fluorescent molecules, which is induced by pore confinement that makes the formation of hydrogen bonds between the hydroxyl moieties of the quenchers and the carbonyl groups of the dendrimer easier.

Therefore, the improvement in sensitivity resulting from the immobilisation of these new probes in a film has allowed the construction of materials with a potential application as detectors for hazardous phenolic compounds.

Experimental Section

Synthesis and characterisation of the dendrimers: All manipulations were carried out by using standard high-vacuum and dry-argon techniques. The solvents were freshly dried and distilled (THF and diethyl ether over sodium/benzophenone, pentane and CH_2Cl_2 over phosphorus pentoxide). ESI mass spectrometry was carried out by using a PE Sciex API 365 instrument. ^{1}H, ^{13}C and ^{31}P NMR spectra were recorded by using Bruker ARX250, AV300 and AV500 spectrometers, respectively. The references for the chemical shifts were 85% H_3PO_4 for ^{31}P NMR spectra and $SiMe_4$ for ^{1}H and ^{13}C NMR spectra. The attribution of ^{1}H and ^{13}C NMR signals was performed by using the *J*-modulated spin echo (J_{mod}), two-dimensional HMBC and HMQC and broadband or continuous-wave ^{31}P decoupling experiments where necessary. The numbering used in the NMR spectra is shown in the Scheme 3. Compounds **2** and **3** are described elsewhere[22] and compound **6** was synthesised according to a previously reported procedure.[16]

Compound 1: The sodium salt of 4-hydroxybenzaldehyde (0.5 g, 3.47 mmol) was added to a solution of hexachlorocyclotriphosphazene (5 g, 14.38 mmol) in THF (400 mL) at 0 °C, and the reaction mixture was stirred at room temperature overnight. After removal of salts by centrifugation, the clear solution was concentrated under reduced pressure and subjected to flash chromatography (pentane/AcOEt, 1:0 to 6:1) to afford **1** as a white powder (65%). Uncorrected m.p. 53 °C; ^{1}H NMR (300.13 MHz, $CDCl_3$): $\delta = 7.42$ (dd, $^3J(H,H) = 8.4$ Hz, $^4J(H,P) = 1.5$ Hz, 2H; C^2–H), 7.98 (d, $^3J(H,H) = 8.4$ Hz, 2H; C^3–H), 10.03 ppm (s, 1H; CHO); ^{13}C{^{1}H} NMR (75.46 MHz, $CDCl_3$): $\delta = 122.13$ (d, $^3J(C,P) = 5.4$ Hz, C^2), 131.66 (d, $^4J(C,P) = 5.4$ Hz, C^3), 134.63 (s, C^4), 153.62 (s, C^1), 190.5 ppm (s, CHO); ^{31}P{^{1}H} NMR (121.49 MHz, $CDCl_3$): $\delta = 11.73$ (t, $^2J(P,P) = 62.4$ Hz, P–O), 22.53 ppm (d, $^2J(P,P) = 62.4$ Hz, P–Cl_2); ESIMS: *m*/*z*: 434 $[M+H]^+$.

Compound 4: A solution of **2** (1.73 g, 4.68 mmol) in THF (5 mL) was added to a solution of **1** (390 mg, 0.91 mmol) in THF (20 mL) at 0 °C, then caesium carbonate (3.04 g, 9.36 mmol) was added and the reaction mixture was stirred at room temperature for two days. After removal of salts by centrifugation, the clear solution was concentrated under reduced pressure and subjected to flash chromatography (hexane/ether to THF) to afford **4** as a yellow powder (86%). ^{1}H NMR (500.33 MHz, $CDCl_3$): $\delta = 2.96$–3.02 (m, 10H; $C^{a'}$–H), 3.85–3.88 (m, 10H; $C^{b'}$–H), 6.94–6.98 (m, 10H; $C^{2'}$–H), 7.07–7.17 (m, 12H; $C^{3'}$–H and C^2–H), 7.30–7.41 (m, 30H; C^m–H and C^p–H), 7.42–7.47 (m, 20H; C^o–H), 7.70–7.73 (d, $^3J(H,H) = 10$ Hz, 2H; C^3–H), 9.95 ppm (s, 1H; CHO); ^{13}C{^{1}H} NMR (125.8 MHz, $CDCl_3$): $\delta = 33.96$ (s, $C^{a'}$), 33.99 (s, C^a), 39.51 (s, $C^{b'}$), 39.54 (s, C^b), 121.10 (m, $C^{2'}$), 121.46 (m, C^2), 128.55 (s, C^m), 128.57 (s, C^m), 128.62 (s, C^i), 128.64 (s, C^i), 129.80 (s, $C^{3'}$), 129.84 (s, $C^{3'}$), 129.89 (s, C^o and C^p), 131.32 (s, C^3), 133.14 (s, C^4), 134.91 (s, $C^{4'}$), 135.08 (s, $C^{4'}$), 136.14 (s, C=C), 136.17 (s, C=C), 149.16–149.31 (m, $C^{1'}$), 155.35–155.41 (m, C^1), 170.53 (s, C=O), 170.54 (s, C=O), 190.95 ppm (s, CHO); ^{31}P{^{1}H} NMR (202.53 MHz, $CDCl_3$): $\delta = 8.47$ ppm (m, P=N); ESIMS (CH_3CN): *m*/*z*: 2098 $[M+H]^+$.

Compound 5: A freshly prepared solution of *N*-methyldichlorothiophosphorhydrazide (0.16 mmol) in chloroform (6 mL) was added to a solution of compound **4** (750 mg, 0.357 mmol) in chloroform (5 mL) at RT. The reaction mixture was stirred overnight at RT, concentrated under reduced pressure to about 4 mL and then precipitated with pentane. The powder was filtered off, dissolved in the minimum amount of THF ($\approx$1 mL) and precipitated with pentane. These washings were repeated three times to afford **5** as a yellow powder (91%). ^{1}H NMR (300.13 MHz, $CDCl_3$): $\delta =$ 2.91–3.01 (m, 10H; $C^{a'}$–H), 3.40 (d, $^3J(H,P) = 14.1$ Hz, 3H; N–Me), 3.78–3.91 (m, 10H; $C^{b'}$–H), 6.88–6.99 (m, 12H; $C^{2'}$–H and C^2–H), 7.07 (d,

^3J(H,H) = 8.4 Hz, 4H; $C^{3'}$–H), 7.15 (d, ^3J(H,H) = 8.4 Hz, 6H; $C^{3'}$–H), 7.27–7.39 (m, 30H; C^m–H and C^p–H), 7.39–7.47 (m, 20H; C^o–H), 7.54 (d, ^3J(H,H) = 8.7 Hz, 2H; C^3–H), 7.69–7.70 ppm (m, 1H; CH=N); $^{13}C\{^1H\}$ NMR (75.46 MHz, $CDCl_3$): δ = 31.77 (d, ^3J(C,P) = 13 Hz, CH_3–N), 33.98 (s, $C^{a'}$), 39.49 (s, $C^{b'}$), 39.54 (s, $C^{b'}$), 121.16 (br s, $C^{2'}$), 121.34 (br s, C^2), 128.52 (s, C^m), 128.55 (s, C^m and C^i), 128.64 (s, C^i), 129.76 (s, C^3), 129.83 (s, $C^{3'}$), 129.87 (s, C^p and C^o), 130.94 (s, C^4), 134.71 (s, $C^{4'}$), 134.82 (s, $C^{4'}$), 134.87 (s, $C^{4'}$), 136.14 (s, C=C), 136.20 (s, C=C), 141.17 (d, ^3J(C,P) = 18.9 Hz, CH=N), 149.26–149.37 (m, $C^{1'}$), 151.99 (br s, C^1), 170.51 (s, C=O), 170.53 ppm (s, C=O); $^{31}P\{^1H\}$ NMR (121.49 MHz, $CDCl_3$): δ = 8.72 (m, P=N), 63.02 ppm (s, P=S).

Compound 7: Azabisdimethylphosphonate (0.742 mg, 1.94 mmol) was added to a solution of **5** (2 g, 0.88 mmol) and caesium carbonate (1.269 g, 3.89 mmol) in THF (20 mL) at 0 °C. The reaction mixture was stirred overnight at RT. Salts were then removed by centrifugation and the clear solution was concentrated under reduced pressure. The residue was then dissolved in the minimum amount of THF (≈1 mL) and precipitated with pentane. The resulting powder was filtered off and the procedure was repeated twice to afford **7** as a yellow powder (83 %). ^{1}H NMR (300.13 MHz, $CDCl_3$): δ = 2.73 (t, ^3J(H,H) = 8.1 Hz, 4H; C^a–H), 2.91–2.99 (m, 10H; $C^{a'}$–H), 3.01 (t, ^3J(H,H) = 8.1 Hz, 4H; C^b–H), 3.18 (d, ^2J(H,P) = 9.0 Hz, 8H; N–CH_2–P(O)(OMe)$_2$), 3.31 (d, ^3J(H,P) = 10.2 Hz, 3H; CH_3–N–P), 3.72 (d, ^3J(H,P) = 10.2 Hz, 24H; P–O–CH_3), 3.81–3.87 (m, 10H; $C^{b'}$–H), 6.90–7.00 (m, 12H; $C^{2'}$–H and C^2–H), 7.01–7.18 (m, 18H; $C^{3'}$–H, $C^{2''}$–H and $C^{3''}$–H), 7.26–7.39 (m, 30H; C^m–H and C^p–H), 7.38–7.47 (m, 20H; C^o–H), 7.59 (d, ^3J(H,H) = 8.4 Hz, 2H; C^3–H), 7.67 ppm (s, 1H; CH=N); $^{13}C\{^1H\}$ NMR (75.46 MHz, $CDCl_3$): δ = 32.92–33.06 (m, CH_3–N–P and C^a), 33.91 (s, $C^{a'}$), 33.97 (s, $C^{a'}$), 39.46 (s, $C^{b'}$), 39.53 (s, $C^{b'}$), 49.43 (dd, ^1J(C,P) = 157.2 Hz and ^3J(C,P) = 7.1 Hz, N–CH_2–P(O)(OMe)$_2$), 52.61–52.70 (m, P–O–CH_3) 58.13 (t, ^3J(C,P) = 7.5 Hz, C^b), 121.11–121.34 (m, $C^{2'}$, C^2 and $C^{2''}$), 128.50 (s, C^m), 128.53 (s, C^m), 128.59 (s, C^i), 128.67 (s, C^i), 129.75–129.85 (m, C^3, $C^{3'}$, C^p and C^o), 130.92 (s, $C^{3''}$), 131.87 (s, C^4), 134.76 (m, $C^{4'}$), 136.13 (s, C=C), 136.45 (s, $C^{4''}$), 138.84 (d, ^3J(C,P) = 14.5 Hz, CH=N), 149.01 (d, ^2J(C,P) = 7.1 Hz, $C^{1''}$), 149.33 (br s, $C^{1'}$), 151.40 (m, C^1), 170.49 ppm (s, C=O); $^{31}P\{^1H\}$ NMR (121.49 MHz, $CDCl_3$): δ = 8.66 (s, P=N), 26.89 (s, P=O), 63.10 ppm (s, P=S).

Compound 8: The sodium salt of 4-hydroxybenzaldehyde (105 mg, 0.718 mmol) was added to a solution of **5** (736 mg, 0.325 mmol) in THF (20 mL) at 0 °C, and the reaction mixture was stirred overnight at RT. Salts were then removed by centrifugation and the clear solution was concentrated under reduced pressure. The residue was then dissolved in the minimum amount of THF (≈1 mL) and precipitated with pentane. The resulting powder was filtered off and the procedure was repeated twice to afford **8** as a yellow powder (83 %). ^{1}H NMR (500.33 MHz, $CDCl_3$): δ = 2.93 (t, ^3J(H,H) = 8.1 Hz, 4H; $C^{a'}$–H), 2.98 (m, 6H; $C^{a'}$–H), 3.37 (d, ^3J(H,P) = 10.9 Hz, 3H; Me–N–P), 3.81 (t, ^3J(H,H) = 8.1 Hz, 4H; $C^{b'}$–H), 3.83–3.87 (m, 6H; $C^{b'}$–H), 6.89–6.99 (m, 12H; $C^{2'}$–H and C^2–H), 7.08 (d, ^3J(H,H) = 8.5 Hz, 4H; $C^{3'}$–H), 7.12–7.15 (m, 6H; $C^{3'}$–H), 7.28–7.29, 7.29–7.45 (2m, 54H; $C^{2''}$–H, C^m–H, C^o–H and C^p–H), 7.56 (d, ^3J(H,H) = 8.6 Hz, 2H; C^3–H), 7.71 (s, 1H; CH=N), 7.85 (d, ^3J(H,H) = 8.6 Hz, 4H; $C^{3''}$–H), 9.92 ppm (s, 2H; CHO); $^{13}C\{^1H\}$ NMR (125.80 MHz, $CDCl_3$): δ = 32.92 (d, ^3J(H,H) = 13.3 Hz, CH_3–N–P), 33.97 (s, $C^{a'}$), 33.99 (s, $C^{a'}$), 39.47 (s, C^b), 39.54 (s, $C^{b'}$), 121.05–121.20 (m, $C^{2'}$), 121.44 (s, C^2), 122.07 (d, ^3J(C,P) = 5.0 Hz, $C^{2''}$), 128.21 (s, C^3), 128.53 (s, C^m), 128.57 (s, C^m), 128.61 (s, C^i), 128.62 (s, C^i), 129.70–129.90 (m, $C^{3'}$, C^p and C^o), 131.47 (s, $C^{3''}$) 133.46 (s, C^4), 134.72 (s, $C^{4'}$), 134.83 (s, $C^{4'}$), 134.91 (s, $C^{4'}$), 136.13 (s, C=C), 139.96–140.15 (m, CH=N), 149.33 (m, $C^{1'}$), 151.76 (m, C^1), 155.15 (d, ^2J(C,P) = 6.9 Hz, $C^{1''}$), 170.51 (s, C=O), 190.76 ppm (s, CHO); $^{31}P\{^1H\}$ NMR (202.53 MHz, $CDCl_3$): δ = 8.66 (m, P=N), 60.69 ppm (s, P=S).

Compound 9: Compound **8** (780 mg, 0.321 mmol) was dissolved in THF (0.8 mL) in presence of a catalytic amount of NEt_3, then dimethyl phosphite (69.6 μL, 0.706 mmol) was added to the solution, and the reaction mixture was stirred overnight at RT. After completion, water was added dropwise and the organic residues were extracted twice with CH_2Cl_2. The organic phase was dried over Mg_2SO_4, filtered and concentrated, then dissolved in the minimum amount of THF (≈1 mL), precipitated with ether/pentane and filtered to remove excess dimethyl phosphite. After evaporation of the residual solvent under reduced pressure, compound **9** was obtained as a yellow powder (85 %). ^{1}H NMR (200.13 MHz, $CDCl_3$): δ = 2.85–3.05 (m, 10H; $C^{a'}$–H), 3.29 (d, ^3J(H,P) = 10.3 Hz, 3H; Me–N–P), 3.50 (d, ^3J(H,P) = 7.0 Hz, 12H; P–O–Me), 3.80–4.10 (m, 10H; $C^{b'}$–H), 4.95 (d, ^2J(H,P) = 9.0 Hz, 2H; HO–C*H*), 6.80–7.70 ppm (m, 83H; CH=N and H_{ar}); $^{13}C\{^1H\}$ NMR (50.323 MHz, $CDCl_3$): δ = 33.96 (br s, CH_3–N–P and $C^{a'}$), 39.52 (s, $C^{b'}$), 53.80 (d, ^2J(C,P) = 7.0 Hz, P–O–Me), 70.03 (d, ^1J(C,P) = 160.9 Hz, HO–CH), 121.05–121.5 (m, $C^{2'}$ and $C^{2''}$), 121.85 (s, C^2), 128.21 (s, C^3), 128.55 (s, C^m), 128.60 (s, C^i), 129.70–129.90 (m, $C^{3'}$, C^p and C^o), 131.70 (d, ^2J(C,P) = 5.7 Hz, $C^{3''}$), 133.41 (s, C^4), 134.69–134.78 (m, $C^{4''}$ and $C^{4'}$), 136.07 (s, C=C), 139.20 (m, CH=N), 149.26 (m, $C^{1'}$ and C^1), 150.81 (d, ^2J(C,P) = 8.9 Hz, $C^{1''}$), 170.49 (s, C=O), 170.54 ppm (s, C=O); $^{31}P\{^1H\}$ NMR (202.53 MHz, $CDCl_3$): δ = 8.70 (m, P=N), 23.06 (m, P=O), 62.16 ppm (s, P=S).

Fluorescence characterisation of the dendrimers in solution: Absorption and fluorescence measurements were performed in solution in distilled dichloromethane at RT by using a Specord 205 spectrophotometer (Analytik Jena AG, Germany) and a PTI model QM-4 spectrofluorimeter (Photon Technology International, USA), respectively. The quenching experiments were also performed in solution in dichloromethane, according to the Stern–Volmer procedure.[32]

Synthesis of the films: Titania mesoporous films were prepared as previously reported in the literature.[14,24] The sol-gel solution was prepared with $TiCl_4$ as the inorganic precursor and Pluronic F127 block copolymer ($HO(CH_2CH_2{-}O)_{106}(CH_2CH(CH_3){-}O)_{70}(CH_2{-}CH_2{-}O)_{106}H$) as the structuring agent in volatile ethanol/water as the solvent. All reagents were used as provided by Sigma–Aldrich. A solution composition of $TiCl_4$/EtOH/H_2O/F127 was adopted, with molar ratios of 1:40:10:0.005. This transparent and slightly viscous solution was homogenised by stirring for 15 min at RT. The solution was then deposited by dip coating the surface of the substrate (100 Si wafer from MEMC Electronic Materials and quartz) at a constant rate of 2.5 mm s^{-1} in a controlled atmosphere. The liquid layers were evaporated at a fixed RH of 15 %, then transferred and aged in a sealed environmental chamber with a fixed RH of 70 % for 18 h. The following thermal treatment was then applied: 24 h at 130 °C and 3 h at 350 °C to increase the density of the amorphous TiO_2, then flash heating at 500 °C for 10 min followed by flash heating at 550 °C for 5 min.

For comparison purposes, mesoporous $(ZrO_2)_x(SiO_2)_{1-x}$ (x = 0.1, 0.2) films were synthesised according to the literature.[33] Physical characterisation (TEM, XRD and EEP) was performed as for titania films.

Functionalisation of titania films: The functionalisation process was carried out by dipping the titania films in a 1 mM solution of dendrimer **7** in dichloromethane. The film was then removed from the solution at a constant rate of 0.16 mm s^{-1} at 40 °C in a temperature-controlled chamber under an air flux to facilitate the solvent evaporation. The as-prepared films were rinsed with dichloromethane to remove the non-bonded dendrimers and then dried under air. The $(ZrO_2)_x(SiO_2)_{1-x}$ (x = 0.1, 0.2) films were soaked in 0.1 mM solutions of dendrimer **9** in THF at RT for 2 h, rinsed with THF and dried under an air flux. The characterisation was performed by using EEP and FTIR, XPS, fluorescence and UV/Vis spectroscopies.

Quenching experiments: The influence of different hydroxyl-containing molecules on the fluorescence properties of the bonded dendrimers was tested. These reactants are displayed in Scheme 2. They were purchased from Sigma–Aldrich and used without further purification. Water, ethanol and 1-pentanol were used as received.

The functionalised films were soaked in a 10 mM solution of the quencher in $CHCl_3$ or EtOH for 10 min (see Table 3 for details) with constant agitation at RT. They were then rinsed with the same organic solvent and dried under air. The fluorescence properties were measured immediately to avoid the effects of humidity on the readings.

Characterisation of the devices: EEP investigations were performed by using a variable-angle ellipsometer 2000U from Woolam in the 500–1000 nm range and by varying the relative humidity of the atmosphere over the TiO_2 films. The porous volume of the TiO_2 films was calculated by using the Brugemann effective medium approximation (BEMA) from the optical properties of the pores and of a TiO_2 reference film that was prepared without structuring agent and that had the same thermal history

as its mesoporous counterpart. The fractions of porous volume filled with water during the analysis were calculated by using BEMA from a mix of dry mesoporous film and completely water-saturated film. All details of the experimental setup and data treatments have been described previously.[34] TEM images were collected by using a JEOL 100 CX II (120 kV) instrument. Samples obtained by scratching the films from the substrate were suspended in ethanol and deposited on carbon–coated copper grids. FTIR measurements were carried out by using a Nicolet Magna 550 spectrometer in transmission mode through the samples deposited on the Si wafer substrates. XPS was performed at room temperature by using a SPECS PHOIBOS 100 hemispherical analyzer with non-monochromatic $Mg_{K\alpha}$ radiation as the excitation source and under a base pressure of $\approx 10^{-9}$ mbar. The samples were glued to the sample holder with silver epoxy. The UV/Vis absorption spectra were recorded by using a UVIKON XL SECOMAM (UVK-Lab) spectrometer directly on the samples deposited on quartz substrates. The steady-state fluorescent behaviour of the samples on quartz was recorded by using a Fluoromax-3 instrument from Horiba Jobin Yvon with the slits fixed at 2 nm. The fluorescence spectrum of each sample was obtained at an excitation wavelength of 373 nm and an emission wavelength of 520 nm, always at RT. No excitation was performed at 290 nm to avoid the decomposition of the dendrimers promoted by the photocatalytic activity of the titania. The samples were water sensitive (see above) so therefore, the initial excitation–emission spectra for the titania films differed slightly.

Acknowledgements

The authors thank the NOE FAME for financial support and integration activities. E.M.-F. thanks the Conselleria d'Empresa, Universitat i Ciència of the Generalitat Valenciana for a postdoctoral fellowship. G.F. is thankful to the European Community for a Ph.D. grant and financial support (Fonds Social Européen).

[1] a) G. R. Newkome, C. N. Moorefield, F. Vögtle, *Dendrimers and Dendrons*, Wiley-VCH, Weinheim, **2001**; b) *Dendrimers and Other Dendritic Polymers* (Eds.: J. M. J. Fréchet, D. A. Tomalia), Wiley, Chichester, **2001**; c) J.-P. Majoral, A. M. Caminade, *Chem. Rev.* **1999**, *99*, 845–880.

[2] A. M. Caminade, J.-P. Majoral, *Acc. Chem. Res.* **2004**, *37*, 341–348.

[3] C.-O. Turin, V. Maraval, A. M. Caminade, J.-P. Majoral, A. Mehdi, C. Reye, *Chem. Mater.* **2000**, *12*, 3848–3856.

[4] G. J. A. A. Soler-Illia, L. Rozes, M. K. Boggiano, C. Sanchez, C.-O. Turrin, A.-M. Caminade, J.-P. Majoral, *Angew. Chem.* **2000**, *112*, 4419–4424; *Angew. Chem. Int. Ed.* **2000**, *39*, 4249–4254.

[5] A. Bouchara, L. Rozes, G. J. A. A. Soler-Illia, C. Sanchez, C.-O. Turrin, A.-M. Caminade, J.-P. Majoral, *J. Sol-Gel Sci. Technol.* **2003**, *26*, 629–633.

[6] a) S. Slomkowski, B. Miksa, M. M. Chehimi, M. Delamar, E. Cabet-Deliry, J.-P. Majoral, A. M. Caminade, *React. Funct. Polym.* **1999**, *41*, 45–57; b) B. Miksa, S. Slomkowski, M. M. Chehimi, M. Delamar, J.-P. Majoral, A. M. Caminade, *Colloid Polym. Sci.* **1999**, *277*, 58–65; c) V. Le Berre, E. Trévisiol, A. Dagkessamanskaia, S. Sokol, A. M. Caminade, J.-P. Majoral, B. Meunier, J. François, *Nucleic Acids Res.* **2003**, *31*, e88/1-e88/8; d) E. Trévisiol, V. Le Berre-Anton, J. Leclaire, G. Pratviel, A. M. Caminade, J.-P. Majoral, J. M. François, B. Meunier, *New J. Chem.* **2003**, *27*, 1713–1719; e) L. Nicu, M. Guirardel, F. Chambosse, P. Rougerie, S. Hinh, E. Trévisiol, J.-M. François, J.-P. Majoral, A. M. Caminade, E. Cattan, C. Bergaud, *Sens. Actuators B* **2005**, *110*, 125–136.

[7] L. Brauge, G. Vériot, G. Franc, R. Deloncle, A.-M. Caminade, J.-P. Majoral, *Tetrahedron* **2006**, *62*, 11891–11899.

[8] a) O. Mongin, T. R. Krishna, M. H. V. Werts, A.-M. Caminade, J.-P. Majoral, M. Blanchard-Desce, *Chem. Commun.* **2006**, 915–917; b) S. Fuchs, H. Otto, S. Jehle, P. Henklein, A. D. Schlüter *Chem. Commun.* **2005**, 1830–1832; c) T. R. Krishna, M. Parent, M. H. V. Werts, L. Moreau, S. Gmouh, S. Charpak, A. M. Caminade, J.-P. Majoral, M. Blanchard-Desce, *Angew. Chem.* **2006**, *118*, 4761–4764; *Angew. Chem. Int. Ed.* **2006**, *45*, 4645–4648.

[9] a) H. Sohn, R. M. Calhoun, M. J. Sailor, W. C. Trogler *Angew. Chem.* **2001**, *113, 2162–2163; Angew. Chem. Int. Ed.* **2001**, 40, 2104–2105; *Angew. Chem. Int. Ed.* **2001**, *40*, 2104–2105; b) X. Wang, H. Zeng, L. Zhao, J. M. Lin, *Talanta* **2006**, *70*, 160–168; c) Y. Wang, K.-M. Wang, G.-L. Shen, R.-Q. Yu, *Talanta* **1997**, *44*, 1319–1327.

[10] a) J. S. Beck, J. C. Vartuli, W. J. Roth, M. E. Leonowicz, C. T. Kresge, K. D. Schmitt, C. T-W. Chu, D. H. Olson, E. W. Sheppard, S. B. McCullen, J. B. Higgins, J. L. Schlenker, *J. Am. Chem. Soc.* **1992**, *114*, 10834–10843; b) G. J. A. A. Soler-Illia, C. Sanchez, B. Lebeau, J. Patarin, *Chem. Rev.* **2002**, *102*, 4093–4138.

[11] a) C. J. Brinker, Y. Lu, A. Sellinger, H. Fan, *Adv. Mater.* **1999**, *11*, 579–585; b) D. Grosso, F. Cagnol, G. J. de A. A. Soler-Illia, E. L. Crepaldi, H. Amenitsch, A. Brunet-Bruneau, A. Bourgeois, C. Sanchez, *Adv. Funct. Mater.* **2004**, *14*, 309–322.

[12] J. D. Bass, D. Grosso, C. Boissiere, E. Belamie, T. Coradin, C. Sanchez, *Chem. Mater.* **2007**, *19*, 4349–4356.

[13] a) C. Sanchez, C. Boissiere, D. Grosso, C. Laberty, L. Nicole, *Chem. Mater.* **2008**, *20*, 682–737; b) M. Kuemmel, D. Grosso, C. Boissiere, B. Smarsly, T. Brezesinski, P. A. Albouy, H. Amenitsch, C. Sanchez, *Angew. Chem.* **2005**, *117*, 4665–4668; *Angew. Chem. Int. Ed.* **2005**, *44*, 4589–4592; c) D. Grosso, C. Boissiere, B. Smarsly, T. Brezesinski, N. Pinna, P. A. Albouy, H. Amenitsch, M. Antonietti, C. Sanchez, *Nature Mater.* **2004**, *3*, 787–792; d) E. L. Crepaldi, G. J. A. A. Soler-Illia, D. Grosso, P. A. Albouy, C. Sanchez, *Chem. Commun.* **2001**, 1582–1583.

[14] E. L. Crepaldi, G. J. d. A. A. Soler-Illia, D. Grosso, F. Cagnol, F. Ribot, C. Sanchez, *J. Am. Chem. Soc.* **2003**, *125*, 9770–9786.

[15] M. Etienne, D. Grosso, C. Boissiere, C. Sanchez, A. Walcarius, *Chem. Commun.* **2005**, 4566–4568.

[16] a) L. Griffe, M. Poupot, P. Marchand, A. Maraval, C.-O. Turrin, O. Rolland, P. Métivier, G. Bacquet, J.-J. Fournié, A.-M. Caminade, R. Poupot, J.-P. Majoral, *Angew. Chem.* **2007**, *119*, 2575–2578; *Angew. Chem. Int. Ed.* **2007**, *46*, 2523–2526; b) M. Poupot, L. Griffe, P. Marchand, A. Maraval, O. Rolland, L. Martinet, F. E. L'Faqihi-Olive, C.-O. Turrin, A.-M. Caminade, J.-J. Fournié, J.-P. Majoral, R. Poupot, *FASEB J.* **2006**, *20*, 2339–2351.

[17] V. Maraval, A. M. Caminade, J.-P. Majoral, J.-C. Blais, *Angew. Chem.* **2003**, *115*, 1866–1870; *Angew. Chem. Int. Ed.* **2003**, *42*, 1822–1826.

[18] V. Chandrasekhar, A. Athimoolam, S. G. Srivatsan, P. S. Sundaram, S. Verma, A. Steiner, S. Zacchini, R. Butcher, *Inorg. Chem.* **2002**, *41*, 5162–5173.

[19] L. M. Lima, F. C. F. de Brito, S. D. de Souza, A. L. P. Miranda, C. R. Rodrigues, C. A. M. Fraga, E. J. Barreiro, *Bioorg. Med. Chem. Lett.* **2002**, *12*, 1533–1535.

[20] P. C. Angelomé, S. Aldabe-Bilmes, M. E. Calvo, E. L. Crepaldi, D. Grosso, C. Sanchez, G. J. A. A. Soler-Illia, *New J. Chem.* **2005**, *29*, 59–63.

[21] D. Prévôté, A. M. Caminade, J.-P. Majoral, *J. Org. Chem.* **1997**, *62*, 4834–4841.

[22] G. Franc, S. Mazères, C.-O. Turrin, L. Vendier, C. Duhayon, A.-M. Caminade, J.-P. Majoral, *J. Org. Chem.* **2007**, *72*, 8707–8715.

[23] a) P. H. Mutin, G. Guerrero, A. Vioux, *J. Mater. Chem.* **2005**, *15*, 3761–3768; b) G. Guerrero, P. H. Mutin, A. Vioux, *Chem. Mater.* **2001**, *13*, 4367–4373.

[24] D. Grosso, G. J. d. A. A. Soler-Illia, E. L. Crepaldi, F. Cagnol, C. Sinturel, A. Bourgeois, A. Brunet-Bruneau H. Amenitsch, P. A. Albouy, C. Sanchez, *Chem. Mater.* **2003**, *15*, 4562–4570.

[25] Y. Sakatani, D. Grosso, L. Nicole, C. Boissiere, G. J. de A. A. Soler-Illia, C. Sanchez, *J. Mater. Chem.* **2006**, *16*, 77–82.

[26] E. Martinez-Ferrero, D. Grosso, C. Boissiere, C. Sanchez, O. Oms, D. Leclercq, A. Vioux, F. Miomandre, P. Audebert, *J. Mater. Chem.* **2006**, *16*, 3762–3767.

[27] N. Adden, L. J. Gamble, D. G. Castner, A. Hoffmann, G. Gross, H. Menzel, *Langmuir* **2006**, *22*, 8197–8204, and references therein.

[28] P. C. Angelomé, G. J. Soler-Illia, *Chem. Mater.* **2005**, *17*, 322–331.

[29] a) T. A. Ostomel, G. D. Stucky, *Chem. Commun.* **2004**, 1016–1017; b) C. Sanchez, B. Lebeau, *MRS Bull. MRS Bulletin* **2001**, *26*, 377–387.
[30] R. M. Silversteing, F. X. Webster, *Spectrometric Identification of Organic Compounds*, 6th ed., Wiley, **1998**.
[31] R. Martinez-Mañez, F. Sancenon, *Coord. Chem. Rev.* **2006**, *250*, 3081–3093.
[32] J. R. Lakowicz, *Principles of Fluorescence Spectroscopy*, Kluwer Academic/Plenum, New York, **1999**.
[33] G. J. de A. A. Soler-Illia, E. L. Crepaldi, D. Grosso, C. Sanchez, *J. Mater. Chem.* **2004**, *14*, 1879–1886.
[34] C. Boissiere, D. Grosso, S. Lepoutre, L. Nicole, A. Brunet-Bruneau, C. Sanchez, *Langmuir* **2005**, *21*, 12362–12371.

Received: April 1, 2008
Published online: July 30, 2008

